WJARR

World Journal of Advanced Research and Reviews

(RESEARCH ARTICLE)

Check for updates

Multispectral imagery for detection and monitoring of vegetation affected by oil spills and migration pattern in Niger Delta Region, Nigeria

Francis Emeka Egobueze [1, *], Eteh Desmond Rowland [2] and Debekeme Silver Ebizimo [2]

[1] Institution of Geoscience Space Technology, Rivers State University of Science and Technology, Nigeria.
[2] Faculty of Science, Department of Geology, Niger Delta University, Wilberforce Island, Bayelsa State, Nigeria.

Abstract

Oil spills in the Niger Delta area can be detected and monitored using this novel technique. Landsat 5 and 8 images were used to assess various vegetation stress, such as Normalized Difference Vegetation Index, Soil Adjusted Vegetation Index, Atmospheric Resistant Vegetation Index, Green Near Infrared and Green Short-wave Infrared, from the spill site in 2019, non-spill site (1992 pre-oil spill) and 2020 post-oil spill events, respectively. There is a substantial difference (p-value <0.005) in the vegetation conditions at the Spill Site and the non-spill Site in 2020 in terms of NDWI, SAVI, ARVI2 and G-NIR and G-SWIR. NDVI, SAVI, ARVI2, G-NIR, G-SWIR, and G-SWIR. There is a very significant difference in vegetation conditions between the pre-spill event and the post-spill event in 2020 (p-value <0.005). The oil spills' migration patterns and flow directions indicate from north to south along the runoff water using SRTM data. The sentinel 1 data revealed visualization of the flooded areas, including water surfaces that are stable around oil pipelines and the surroundings, using calibration threshold and the RGB band method to distinguish flooded areas from permanent water bodies. This was used to map areas affected by the oil spill on land and water bodies for proper environmental assessment before and during the flood of the oil spill environment. Multi spectral imagery is therefore a veritable tool for detection, response and monitoring of oil spills from pipelines.

Keywords: Oil spill; Remote Sensing; Vegetation indices; SRTM; Flood

1. Introduction

"Oil spill" refers to the unintentional discharge of a liquid petroleum hydrocarbon into the environment, especially into the marine ecosystem, as a result of human activities [1]. The use of multispectral imagery can be employed in oil spill detection and monitory including oil migration and spreading during flood. Oil spill has continually been a fundamental challenge in the Niger Delta Region by means of pollution in the environment with hydrocarbon and is a basic global natural issue. The utilization of remote sensing in detection of hydrocarbon spill locations, and monitoring of remediation sites dates ack to the 1970s, at first, was the use of aerial photographs [2]. Ultraviolet (UV), thermal infrared, and microwave sensors have been evaluated for their ability to detect oil contamination during current research [3,4]. Sensors, information inquiry, and communication advancements in geospatial technology have introduced new approaches. Satellite and airborne radar, LIDAR, hyper-spectral, and multispectral sensors are just a few of the remote sensing technology images that may be used to monitor oil pipelines or spills [5]. The identification of hazardous liquid leakage stress in plants, the quantification of pollution and stress levels, and the monitoring of contaminated locations after remediation have all been accomplished using remote sensing pictures [6]. Using Landsat 7 Enhanced Thematic Mapper (ETM) images, researchers [7] observed characteristics of weathered oil suspended in the water column with brilliant contrast and oil film floating on the sea surface with dark contrast. For example, environmental conditions may cause stress and dehydration in plants, both of which can be harmful [8]. Reduced

transpiration is caused by a reduction in the plant's water potential. This includes both natural and man-made factors, which might cause damage to plants [9]. Abiotic stressors include temperature, water, chemical, and mechanical stresses on plants, which include disorder, infection, competition, and herbivory [10]. Oil and gas development and extraction, in the Niger Delta region, may be the primary cause of stress on vegetation [11]. Plant removal is part of the site selection process, as well as the building and management of a facility [12, 13]. Chemical elements and other contaminants that are discharged into the soil over the course of operations may have an impact on vegetation [14]. Monitoring of environmental stressors such as oil spills may be confirmed by using previous knowledge of the oil facility locations, oil spill file, and GPS area of the affected sites.

"Oil spill" refers to the unintentional discharge of a liquid petroleum hydrocarbon into the environment, especially into the marine ecosystem, as a result of human activities [1]. The use of multispectral imagery can be employed in oil spill detection and monitory including oil migration and spreading during flood. Oil spill has continually been a fundamental challenge in the Niger Delta Region by means of pollution in the environment with hydrocarbon and is a basic global natural issue. The utilization of remote sensing in detection of hydrocarbon spill locations, and monitoring of remediation sites dates ack to the 1970s, at first, was the use of aerial photographs [2]. Ultraviolet (UV), thermal infrared, and microwave sensors have been evaluated for their ability to detect oil contamination during current research [3,4]. Sensors, information inquiry, and communication advancements in geospatial technology have introduced new approaches. Satellite and airborne radar, LIDAR, hyper-spectral, and multispectral sensors are just a few of the remote sensing technology images that may be used to monitor oil pipelines or spills [5]. The identification of hazardous liquid leakage stress in plants, the quantification of pollution and stress levels, and the monitoring of contaminated locations after remediation have all been accomplished using remote sensing pictures [6]. Using Landsat 7 Enhanced Thematic Mapper (ETM) images, researchers [7] observed characteristics of weathered oil suspended in the water column with brilliant contrast and oil film floating on the sea surface with dark contrast. For example, environmental conditions may cause stress and dehydration in plants, both of which can be harmful [8]. Reduced transpiration is caused by a reduction in the plant's water potential. This includes both natural and man-made factors, which might cause damage to plants [9]. Abiotic stressors include temperature, water, chemical, and mechanical stresses on plants, which include disorder, infection, competition, and herbivory [10]. Oil and gas development and extraction, in the Niger Delta region, may be the primary cause of stress on vegetation [11]. Plant removal is part of the site selection process, as well as the building and management of a facility [12, 13]. Chemical elements and other contaminants that are discharged into the soil over the course of operations may have an impact on vegetation [14]. Monitoring of environmental stressors such as oil spills may be confirmed by using previous knowledge of the oil facility locations, oil spill file, and GPS area of the affected sites.

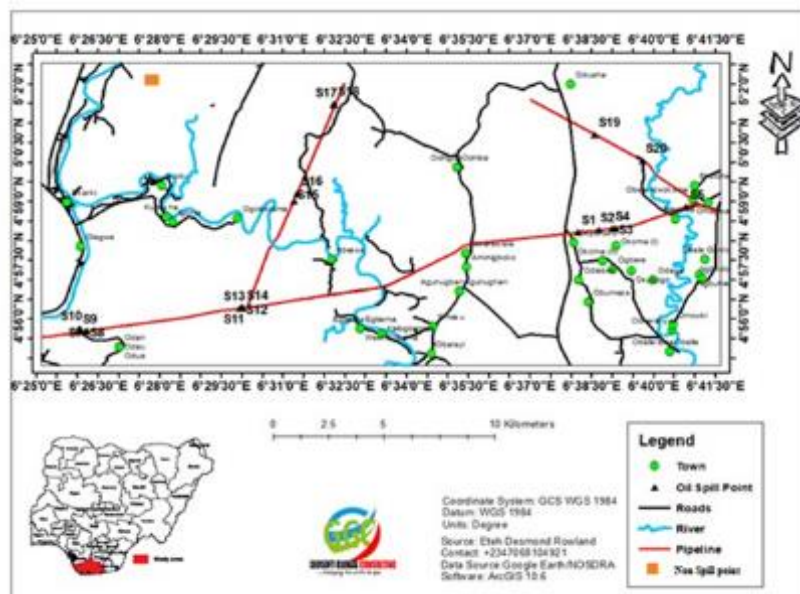## 1.1. Physiography and Geology of the Study Area

Figure 1 Study location map

The research site is located between the coordinates 4°56'0" N and 6°41'30" E. Typically, the geography is low-lying, with elevations varying from sea level on the location's southwest edge to 39 m [15] or so inland in comparable areas.

The region has an average rainfall of 2,899mm and a temperature of 26.7°C. Many streams and creeks drain the region, including Kolo Creek, which is connected to the Nun and Orashi rivers. The SPDC and Agip Oil Company hold multiple hydrocarbon flow stations in the research region, making road access possible. Within the Niger Delta Basin, the Benin Formation, an Eocene-aged formation, lies under quaternary deposits in most locations. The Benin Formation's sands and sandstones are generally coarse to fine-grained, granular in texture, and unconsolidated. In the Benin Formation, clean water-bearing continental sand and gravels predominate with intercalations of clay and shale indicative of depositional environments such as lagoons and fluvio-lacustrine/deltaic [16]. The Benin Formation's clayey intercalation gives origin to the Niger Delta's multi-aquifer system, with the shallow unconfined aquifer occurring at depths ranging from 20 meters to 40 meters throughout the region [17].

2. Material and methods

2.1. Data collection

A total number of 20 oil spills sites was gotten from Nigeria Oil Spill Detection and Response Agency (NOSDRA) http://nosdra.gov.ng achieves at https://oilspillmonitor.ng site with 19 spill locations in 2019 and 1 in 2020 along Shell and Agip oil pipeline within the study area (see Figures 2). Other data collected are Shuttle Radar Topographical Mission (SRTM) downloaded from https://dwtkns.com/srtm30m, Landsat 5 Imagery in 1992, Landsat 8 imagery in 2020 and Sentinel 1 data in 2019 along with administrative map from where political boundaries and roads were obtained and digitized from a high-resolution image of about 3m from Google Earth (Table 1).

Table 1 List of Data Satellite Data collected

Satellite Data	Date	Spatial Resolution (m)	Source
SRTM	22/11/2000, 1-ARC second	30	https://dwtkns.com/srtm30m
Landsat 5	09/01/1992 Path: 189, Row: 57	30	https://earthexplorer.usgs.gov/
Landsat 8	6/1/2020 Path: 189, Row: 56	30	https://earthexplorer.usgs.gov/
Sentinel 1	25/7/2019	10 m	https://scihub.copernicus.eu
Sentinel 1	10/11/2019	10m	https://scihub.copernicus.eu
Google Earth Imagery	06/02/2020	3	https://google.com/earth

Table 2 Information on oil spill data for the study site

Sample	Company	Incident Date	Lat	Long	State	Barrels
S1	SPDC	2019-08-02	4.970361111	6.636194444	Rivers states	unknow
S2	SPDC	2019-09-05	4.971311111	6.644530556	Rivers states	154
S3	SPDC	2019-07-29	4.972166667	6.651277778	Rivers states	31
S4	SPDC	2019-05-19	4.9671	6.651319444	Rivers states	3
S5	SPDC	2019-02-27	4.981077778	6.679972222	Rivers states	0.62
S6	SPDC	2019-01-09	4.928261111	6.437030556	Rivers states	4
S7	SPDC	2019-02-09	4.928319444	6.437138889	Rivers states	290
S8	SPDC	2019-08-25	4.9283	6.437088889	Rivers states	243
S9	SPDC	2019-07-31	4.928277778	6.434361111	Rivers states	Unknow
S10	SPDC	2020-01-20	4.929788889	6.434361111	Rivers states	247

S11	SPDC	2019-07-22	4.938	6.499277778	Rivers states	Unknow
S12	SPDC	2019-12-11	4.93855	6.500080556	Rivers states	3
S13	SPDC	2019-06-17	4.938138889	6.500238889	Rivers states	267
S14	SPDC	2019-07-17	4.938222222	6.500388889	Rivers states	289
S15	NAOC	2019-01-02	4.983694444	6.521083333	Rivers states	0.63
S16	NAOC	2020-01-06	4.986972222	6.522388889	Rivers states	72
S17	NAOC	2019-01-04	5.024444444	6.537305556	Rivers states	unknow
S18	NAOC	2018-09-11	5.025	6.5375	Rivers states	500
S19	SPDC	2019-06-28	5.01185	6.643080556	Rivers states	2
S20	SPDC	2019-10-11	5.000916667	6.662222222	Rivers states	73

Limitation

Niger Delta area cloud cover in 2019 prevented Landsat 8 from getting adequate access to oil spill data from the Nigeria Oil Spill Detection and Response Agency (NOSDRA).

2.2. Data processing

The height information from SRTM DEM (Digital Elevation Model), drainage channel, and drainage basin in hydrology tools for oil spill migration was generated using the Arc GIS 10.6 spatial analyst extension. Before processing the Vegetation stress such as NDVI, SAVI, ARVI2, G-G-NIR, the data was imported into Microsoft Excel and converted to degree decimal before being transferred to Geographical Information System environment in Data Base Format to produce sample location map and then superimposed on the Digital Elevation map and Drainage channel map. The statistical analysis was performed using SPSS version 25.

2.3. SAR Sentinel-1 Data Processing

Sentinel 1 data has not been used particularly in the region for this purpose because of flooding in the past 20 years. Therefore, Snap 6.0 software was used to process sentinel 1 data. Snap software was launched and image zone imported to select the area of interest, subset, multi-look, calibrate, covert linear to/from dB for better visualization. Terrain correction was performed in other for geolocation of the image, contact stretch was applied to pick cell on both images to separate land from permanent water bodies from flooded area. Both images were layer stacked and RGB combination was applied [18], However, calibration threshold technique [19] was used also you to separate land from permanent water bodies from flooded area before exporting the images and importing into ArcGIS environment for proper visualization and superimposed on the spill environment for further analysis to estimate the water bodies in the flooded area.

2.4. Vegetation Indices

Landsat 7 and 8 imageries have been utilized several times for detecting oil spills and their influence on plant stress due to the usage of broadband multispectral data derived vegetation indices. This study focuses on the usage of five Landsat 5 and 8 sensors' vegetation stress data.

Table 3 Spectral bands in Landsat 8 for vegetation indices

Band no	Description	Wavelength (µm)	Resolution (m)
2	visible blue	0.450 to 0.515	30
3	visible green	0.525 to 0.6	30
4	visible red	0.630 to 0.68	30
5	Near-Infrared	0.845 to 0.885	30
6	Short-wave infrared I	1.56 to 1.66	30

Table 4 Spectral bands in Landsat 5 for vegetation indices

Band no	Description	Wavelength (μm)	Resolution(m)
1	visible blue	0.450 to 0.515	30
2	visible green	0.525 to 0.6	30
3	visible red	0.630 to 0.69	30
4	Near-Infrared	0.77 to 0.90	30
5	Short-wave infrared 1	1.55 to 1.75	30

2.5. Atmospheric correction

Using the Landsat-8 metadata file, equations 1 and 2 offer the formulae for atmospheric correction from Digital Number (DN) to Top of Atmosphere (TOA) rescaling coefficients.

$$p\lambda = M_p Q_{cal} + A_p \dots\dots\dots\dots\dots\dots\dots\dots\dots(1)$$

The planetary reflectance without adjustment for the sun angle is denoted by the symbol ρλ' TOA. Band-specific multiplicative rescaling factor from the metadata is denoted by Mρ. A band-specific additive rescaling factor from the metadata is denoted by Aρ, Quantized and calibrated standard product pixel values (DN) is denoted by Qcal.

TOA reflectance corrected for the sun angle is:

$$p\lambda = \frac{p\lambda}{\cos(0sz)} = \frac{p\lambda}{\cos(0se)} \dots\dots\dots\dots\dots\dots\dots\dots\dots (2)$$

2.6. Normalized Difference Vegetation index

It has been shown that the NDVI has distinct spectral properties that may be used to assess vegetation stress. For example, the red band in the visible spectrum is sensitive to variations in chlorophyll concentration, but the near-infrared spectrum has the ability to identify different plant species and conditions. The index has been effectively utilized for evaluating plant cover, and it is still believed to have significant promise for use in environmental monitoring due to its cheap cost when compared to hyperspectral data, which makes it an attractive alternative [20, 21].

NDVI = (RNIR – RRED) / (RNIR+RRED) ....(3)

2.7. Soil Adjusted Vegetation Index

When Huete et al.,[22] established the SAVI index, they included an adjustment factor for canopy backdrop and atmospheric conditions to account for the noise seen in the NDVI. This index is important in addressing the soil and atmospheric effects of a given situation [23].

SAVI = ((RNIR – RRED) / (RNIR + RRED + 0.5)) x (1 + 0.5) .... (4)

2.8. Atmospheric Resistant Vegetation Index 2

As a result, the ARVI2 index is more responsive to chlorophyll concentrations over a wider range than the ARVI1 index. Both NDVI and ARVI2 are sensitive to the amount of vegetation present and the pace at which sunlight is absorbed by the plant [12, 13].

ARVI2 = -0.18 + 1.17 x (RNIR – RRED/RNIR + RRED) .... (5)

2.9. Green-Near Infrared

To calculate the G-NIR index, we simply add up the reflectance values for green and near infrared light. Plant vigor may be assessed using the green band, while the NIR band provides information on the interior structure of plants [14]. It has also shown the ability to distinguish between oil spill-affected and unaffected vegetation in terms of both space and time [24].

$$\text{G-NIR} - (\text{RGREEN} - \text{RNIR}) / (\text{RGREEN} + \text{RNIR}) \dots\dots\dots\dots\dots\dots\dots\dots\dots\dots (6)$$

2.10. Green-Short-wave Infrared

In plants, the G-SWIR index is able to detect and forecast nitrogen levels [25]. It is possible that G-SWIR might be used to identify changes in vegetation affected by an oil spill since SWIR can distinguish between the moisture content of soil and plants [26].

$$\text{G-SWIR} - (\text{RGREEN} - \text{RSWIR}) / (\text{RGREEN} + \text{RSWIR}) \dots\dots\dots\dots\dots\dots\dots\dots\dots (7)$$

3. Results and discussion

The differences in vegetation stress between 2020 spill locations and non-spill sites in 1992, was determined by the findings of a study. Research of the significant shift in vegetation indexes between 1992 and 2020 was carried out further. From pre-spill to post-spill, vegetation conditions at the spill and non-spill sites were studied in Table 5.

Table 5 A comparison of p-value from paired t-test analysis in SS of 1992 vs 2020

Index	Change	P-Value
NDVI 1992 – NDVI 2020	0.15	***
SAVI 1992 – SAVI 2020	0.07	ns
ARVI2 1992 – ARVI2 2020	0.15	***
G-NIR 1992 –G-NIR 2020	-0.10	***
G-SWIR 1992 – G-SWIR 2020	0.37	***

Table 6 Analysis of change detection using paired t-test statistics of means of vegetation indices at the Control Site in 1992 vs SS in 1992, 2020

INDEX	CHANGE	P-VALUE	INDEX	CHANGE	P-VALUE
NDVI_C - NDVI1992	0.37	***	NDVI_C - NDVI2020	0.52	***
SAVI_C - SAVI1992	0.40	***	SAVI_C - SAVI2020	0.47	***
ARVI2_C - ARVI21992	0.43	***	ARVI2_C - ARVI22020	0.58	***
GNIR_C - GNIR1992	0.98	***	GNIR_C - GNIR2020	0.88	***
GSWIR_C - GSWIR1992	0.76	***	GSWIR_C - GSWIR2020	1.13	***

****p-value < 0.0001; *** p-value < 0.005; ** p-value < 0.01; * p-value < 0.05; ns p-value ≥ 0.05; Key: ****Highly significant; ***Highly significant; **Very significant; *Significant; ns Not significant

3.1. Environmental assessment oil spill on vegetation

Based on data from January 9, 1992 and January 6, 2020, the study sought to investigate whether vegetation affected by oil spills in 2019 responds spectrally differently to the non-spill location. On January 6, 2020, Table 3 will show low indices at the spill location and high indices at the non-spill site A comparison of the vegetation indices at spill and non-spill is shown in Figure 2 and 3. There were no significant differences found between the vegetation indices at spill and non-spill locations, according to the t-test results shown in Table 3. NDVI, SAVI, ARVI2, G-NIR, and G-SWIR were shown to have a greater level of significant difference of P>0.005 between the spill and non-spill locations, respectively.
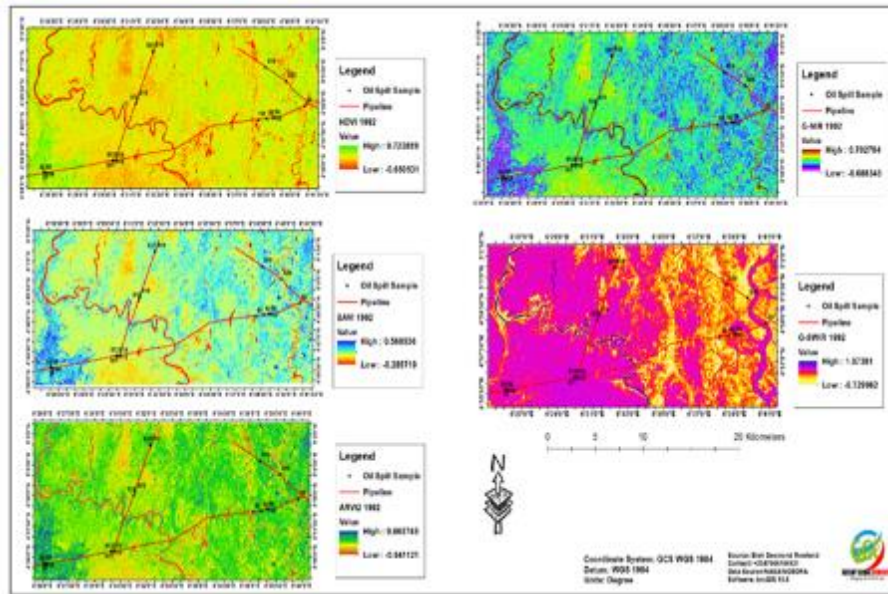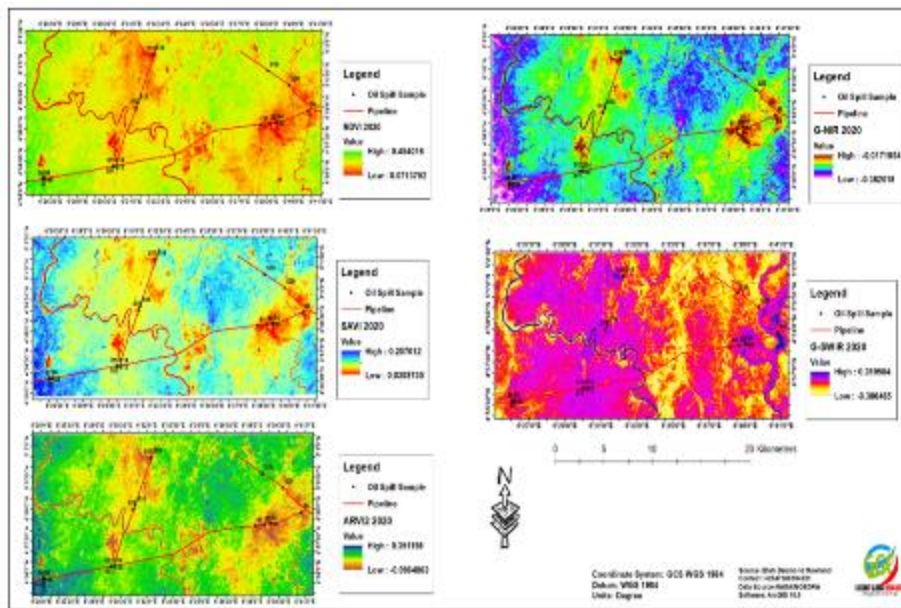
Figure 2 Vegetation Indices for 1992

Figure 3 Vegetation Indices for 2020

3.2. Vegetation Indices on change detection at the Spill Site and Non-Spill Site using oil spill monitory

In Table 3, vegetation indices from Landsat 5 and Landsat 8 images taken on January 9, 1992 and January 6, 2020 were statistically compared at both spill locations. A significant difference between spill and non-spill vegetation was shown to exist in the indices of vegetation such as NDVI, SAVI, ARVI2, G-NIR, and G-SWIR with p values 0.005 in the study. According to the pre-spill picture of January 9, 1992, NDVI, SAVI, ARVI2, G-NIR and low G-SWIR were all higher in reflectance in the post-spill image of January 6, 2020. Spill and non-spill locations were found to have significantly different G-SWIR values, with a p value 0.005 for NDVI, SAVI, ARVI2 and G-NIR, respectively. Further explanation of vegetation status at spill site before and after oil spill is provided by NDVI, SAVI ARVI2, G-NIR, and G-SWIR, which showed a higher level of significant difference in 1992, as well as in Table 3 with various changes in NDVI 1992 and 2020, which is 0.15 spectral reflectance (along with other indices) at Table 3. Thus, plant stress-induced spectral changes at these locations in 1992 (before to the disaster) and 2020 (after the spill) clearly reveal oil-spill-affected and oil-spill-unaffected vegetation.

3.3. Terrain analysis affected by oil spill

The Digital Elevation Model of the study area ranges from 4.00 m to 39.00 m (Figure 5). The southern part of the study area cutting across several communities in the region where farmlands and fish ponds are located were largely due to peculiar environment made up of mangrove forest. When oil spill occurs its proven to spread if adequate environmental protection measures including containment using barriers, recovery and cleanup are not carried out thereby impacting many areas mostly water channels that are linked to one another. This results in display of low elevation (Figure 5-white and blue) indicating that such areas are most likely the first to be overcome by flood waters [15, 27] . It therefore indicates that during flood season spill is likely to affect more areas in the region. The north-western and the eastern parts (Figure 5-brown and yellow areas) of the study area are observed to have higher elevation indicating that flood waters would require greater height to overcome these areas as seen in see Figure 6 which corresponds to findings by Eteh et al [15].
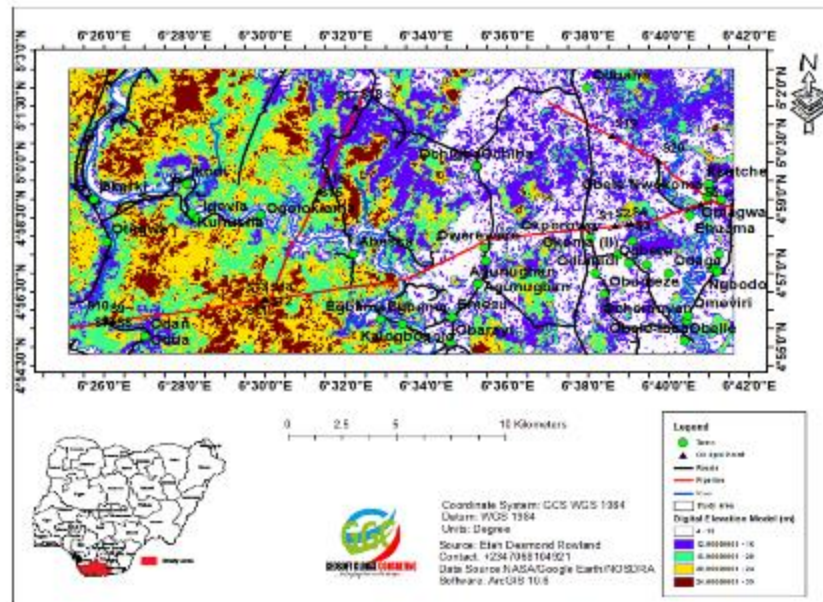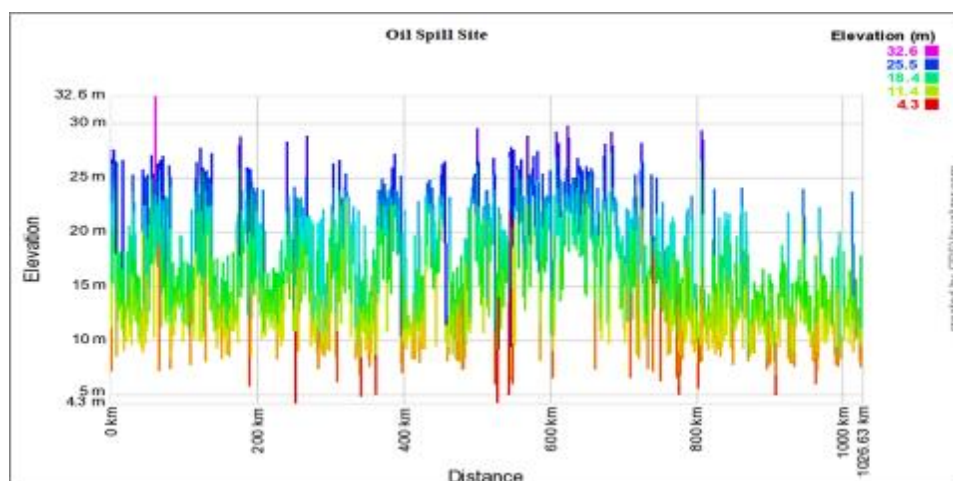

Figure 4 Digital Elevation Model of Study area

Figure 5 Digital Elevation Model Profile of oil spill site

3.4. Effect Oil Spill On Flood

In figure 6, the graph shows the characteristic of points, which were obtained to provide the behavior of the radar on different surfaces and estimate the significant difference in means on water surface for July and November in 2019. The

calibration threshold separated the land from water bodies sheet through the interpretation of chart coupled with the relationship between polarizations and characteristic chart for each of radar image as observed. The RGB bands method was used to distinguish between more flooded areas and permeant waterbodies Figure 7. The image before and during the flood were combine and the Red-band appear as red which reflect the area has high radar responds on the red channel but a low radar respond in the green and blue channel over the sounding area were, we have no flood area, showing the presence of tones of gray as backscatter in Figure 7. The different results obtained in July and November 2019 for Co-polarizations (VV) can be seen in Figure in Figure 7. The combination reveals the visualization of the flooded areas including water surfaces that are stable around oil pipeline and the surroundings. The affected area could be mapped out as farmland, fish pond including contamination area before the flood and during flood for proper environmental assessment and for cleanup up process. This was used to investigate the water quality and air quality before the flood and during flood on oil spill environment. The areas, with intermediate intensity values in which there have been hardly any variations, are consolidated in blue tones as backscatter. The light pink tones are characteristic of areas with high humidity while the red shows the flood surfaces in which the water has completely flooded within study area.
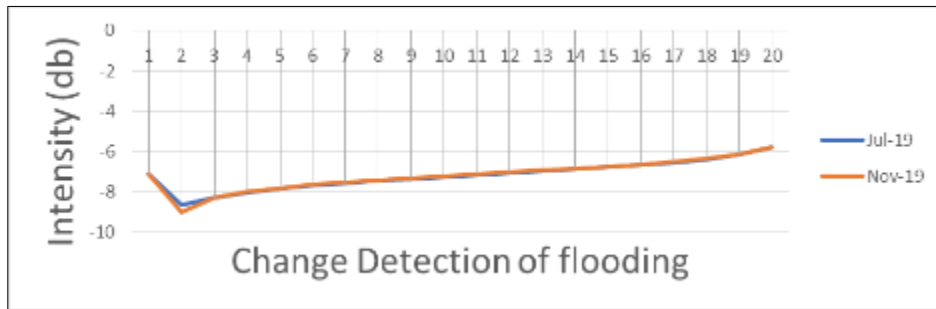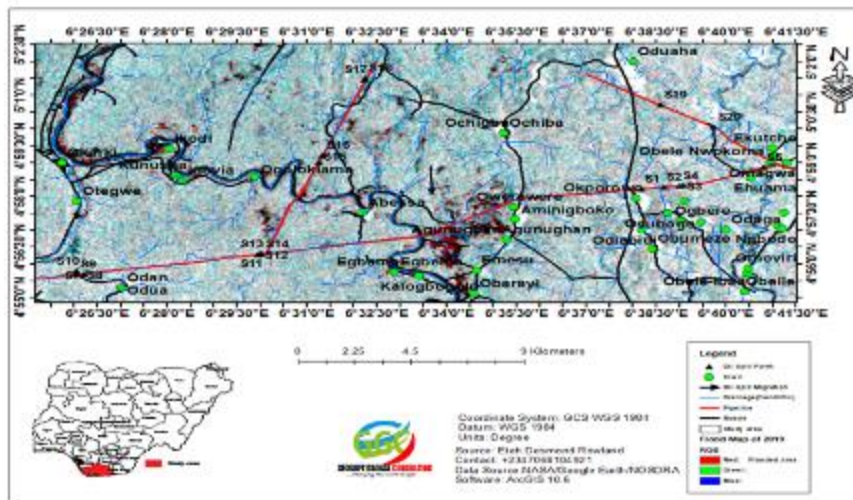

Figure 6 Change detection of flooding

Figure 7 Oil Spill site flooded area map of 2019 November

3.5. Migration of oil spills

From Shuttle Radar Topographical Mission SRTM, the results reveal that oil spills migration patterns flow along the runoff water, considering the nature of the terrain were the oil pipeline are layed (Figure 8) if flood occurs, a lot of communities especially the riverine communities will be affected due to the nature of the terrain and the drainage system within the study area is observed to be dendritic in nature [28,29] so when oil spill occurs, it flows in the direction moving from the north to the south (Figure 8) along the drainage channel but in dry season it is observed to settle within the catchments areas/sub-basins where it identified in a single watershed indicating that the study area has an adequate drainage system. This highly connected drainage system is present within the study area, the absence and inability to obey and enforce environmental laws and practices have led to the blockage of most natural drainage within the settlement, farmland and pounds. The drainage pattern within the study also reveals that water enters into Orashi River from the upland including creeks like Taylor creek and kolo creek (Figure 7).
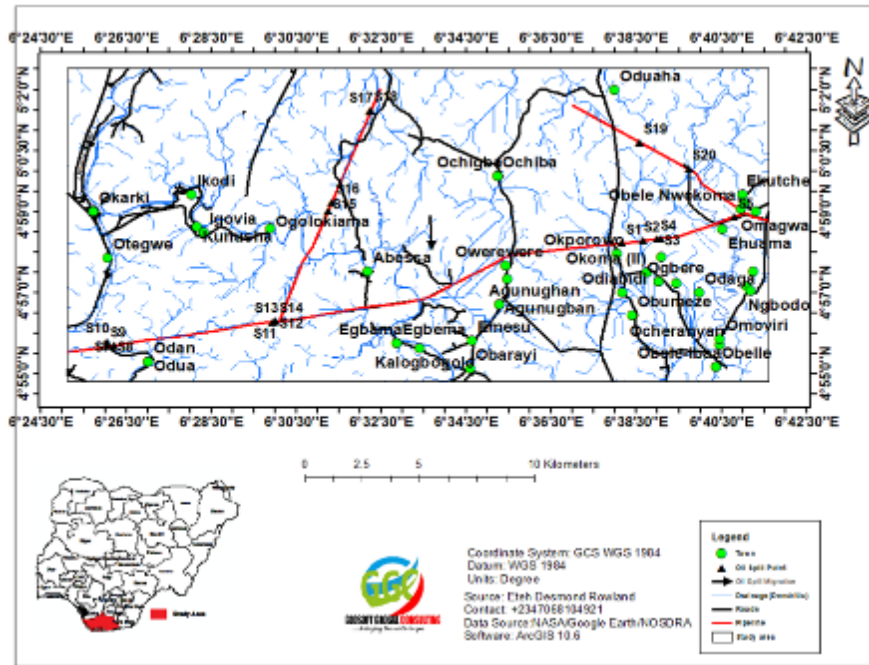
Figure 8 Oil Spill site migration map of Study area

3.6. Consequence for oil spill detection and monitoring

Oil spill planning and response procedures are based on the ability to accurately categorize remotely sensed data. Methods that are costly, time demanding, confined in geographical and temporal coverage, or inadequate for detecting oil spills in mangrove forests have been used in a variety of studies and recommendations [30, 4]. These methods have now been deemed unsuitable for detecting oil spills and recommending acceptable containment and clean-up strategies in the affected regions. Mangrove forests are essential to the ecosystem and must be handled carefully. A new strategy, developed in this research, has been used to keep oil spill detection effective while lowering costs and increasing the spatial and temporal scope of post-event monitoring. Results from this research are critical to the oil business, as well as government and non-governmental organizations responsible for protecting the natural environment. Local governments might benefit from the low-cost and effective use of space technology to monitor oil plants. According to the findings of this research, oil spill detection may be coordinated so that information can be made available to local authorities. Oil spill response in mangrove environments may benefit from this method.

As a result of this research, data on post-spill information and the remediation/clean-up procedures of the affected locations are presented. There are two ways in which we may distinguish between vegetation that has been impacted by the usage of the oil spill and those that have not been impacted.

4. Conclusion

The oil industry in Nigeria is responsible for environmental degradation in the Niger Delta oil producing zones, and remote sensing methods are utilized to analyze and monitor vegetation impacted by oil spills. There were significant differences in vegetation indexes between the Spill Site and Non-Spill Site as a consequence of the results of a t-test. According to the findings, the Spill Site and Non-Spill Site were shown to have a greater degree of significant difference in five vegetation indices, namely Normalized Difference, Soil Adjusted, Atmospheric Resistant, Green Near Infrared, and Green Short-wave Infrared. NDVI, SAVI, ARVI2, G-NIR, and low G-SWIR in the pre-spill picture of 9/01/1992 and the post-spill image on 6/1/2020 1992 reveal a very significant difference with p-value 0.005 between Spill Site and Non-Spill Site based on NDVI, SAVI, ARVI2, G-NIR, and low G-SWIR. The obtain data of Shuttle Radar Topographical Mission analysis in the area show low attitude raining from 4 m to 39 m making the area to have a lot of subbasin with a single watershed thereby oil spills migration patterns flow along the runoff water in oil pipeline rout ,if flood occur, a lot of communities especially the riverine communities will be affected due to the nature of the terrain and the drainage system within the study area is observed to be dendritic in nature (Goudie 2005, Arthur, 1967) so when oil spill occurs, it flow direction moving from the north to the south (Figure 8) along the drainage channel but in dry season it is observed to settle within the catchments areas/subbasins area. The calibration threshold separated the land from

waterbodies sheet through the interpretation of Histogram and the RGB bands method was used to distinguish between flooder area and permeant waterbodies Figure 7 to map out communities that will belikely affected by oil spill during dry and rainy season using sentinel 1 Aperture Radar data using image in before the flood and image during the flood for proper assessment of oil spill detection and monitory in the Niger Delta region.

Compliance with ethical standards

Disclosure of conflict of interest

The authors declare that there is no conflict of interest regarding the publication of this article.

References

[1] NOAA Ocean Media Center. "Hindsight and Foresight, 20 Years after the Exxon Valdez Spill". NOAA. Retrieved 2010-04-30.

[2] Casciello, D., T. Lacava, N. Pergola, and V. Tramutoli: Robust Satellite Techniques for oil spill detection and monitoring using AVHRR thermal infrared bands, International Journal of Remote Sensing, 2011, 32:14, 4107-4129 doi :10.1080/01431161.2010.484820

[3] Brekke, C., and A. H. S. Solberg. "Oil Spill Detection by Satellite Remote Sensing." Remote Sensing of Environment. 2005, 95 (1): 1–13. doi:10.1016/j.rse.2004.11.015.

[4] Fingas, M. F., and C. E. Brown. "Review of Oil Spill Remote Sensing." Spill Science & Technology Bulletin.1997, 4 (4): 199–208. Doi : 10. 1016/S1353-2561(98)00023-1.

[5] Jha, M. N., J. Levy, and Y. Gao. (2008). "Advances in Remote Sensing for Oil Spill Disaster

[6] Van der Werff, H., M. van der Meijde, F. Jansma, F. van der Meer, and G. J. Groothuis. "A Spatial-Spectral Approach for Visualization of Vegetation Stress Resulting from Pipeline Leakage." Sensors 2008, 8 (6): 3733–3743. Doi : 10. 3390/s8063733.

[7] Zhao, M., M.-L. Timmermans, S. Cole, R. Krishfield, A. Proshutinsky, and J. Toole Characterizing the eddy field in the Arctic Ocean halocline, J. Geophys. Res. Oceans,2014, 119, 8800– 8817, doi:10.1002/2014JC010488

[8] Carter, G. A. "Responses of Leaf Spectral Reflectance to Plant Stress." American Journal of Botany 1993, 80 (3): 239–243. Doi :10.2307/2445346.

[9] Yim, U. H., S. Y. Ha, J. G. An, J. H. Won, G. M. Han, S. H. Hong, M. Kim, J. H. Jung, and W. J. Shim. "Fingerprint and Weathering Characteristics of Stranded Oils after the Hebei Spirit Oil Spill." Journal of Hazardous Materials2011, 197: 60–69. doi:10.1016/j.jhazmat.2011.09.055.

[10] Schulze ED, Beck E, Hohenstein KM. Environment as stress factor: stress physiology of plants. Plant Ecology. 2005;702:7-11.

[11] United Nations Environment Programme (UNEP), Environmental Assessment of Ogoniland (Nairobi:UNEP, 2011), available at http://postconflict.unep.ch/publications/OEA/UNEP_OEA.pdf [UNEP Report].

[12] Gitelson, A. A., Y. J. Kaufman, and M. N. Merzlyak. "Use of a Green Channel in Remote Sensing of Global Vegetation from EOS-MODIS." Remote Sensing of Environment.1996, 58 (3): 289–298. doi:10.1016/S0034-4257(96)00072-7.

[13] Kaufman, Y. J., and D. Tanre. "Atmospherically Resistant Vegetation Index (ARVI) for EOSMODIS." IEEE Transactions on Geoscience and Remote Sensing 1992, 30 (2): 261–270. doi:10.1109/ 36.134076.

[14] Sripada, R. P., R. W. Heinigerb, J. G. Whitec, and A. D. Meijer. "Aerial Colour Infrared Photography for Determining Early In-Season Nitrogen Requirements in Corn." Agronomy Journal.2005, 98 (4): 968–977. doi:10.2134/agronj2005.0200.

[15] Eteh Desmond Rowland, Egobueze Emeka Francis, & Omonefe, Francis. Determination of Flood Hazard Zones Using Geographical Information Systems and Remote Sensing Techniques: A Case Study in Part Yenagoa

Metropolis. Journal of Geography, Environment and Earth Science International, 2019, 21(1), 1-9. doi.org/10.9734/jgeesi/2019/v21i130116

[16] Usman Shehu Onoduku. "Chemistry of Maiganga Coal Deposit, Upper Benue Trough, North Eastern Nigeria". Journal of Geosciences and Geomatics. 2014, 2(3):80-84. doi: 10.12691/jgg-2-3-2.

[17] Reijers, T.J.A Stratigraphy and Sedimentology of the Niger Delta. Geologos, The Netherlands, 2011, 17(3), p.133-162. doi: 10.2478/v10118-011-0008-3

[18] Tavus, B., Kocaman, S., Gokceoglu, C., and Nefeslioglu, H. A. CONSIDERATIONS ON THE USE OF SENTINEL-1 DATA IN FLOOD MAPPING IN URBAN AREAS: ANKARA (TURKEY) 2018 FLOODS, Int. Arch. Photogramm. Remote Sens. Spatial Inf. Sci, 2018, XLII-5, 575–581, doi.org/10.5194/isprs-archives-XLII-5-575-2018.

[19] Martinis and Rieke, "Backscatter analysis using multi-temporal and multi-frequency SAR data in the context of flood mapping at river saale "Germany Remote Sensing, 2015, 7 (6) (2015), pp. 7732-7752, doi:10.3390/rs70607732

[20] Rouse, J. W. Jr., R. H. Haas, J. A. Schell, and D. W. Deering. (1973). "Monitoring the Vernal Advancement and Retrogradation (Green Wave Effect) of Natural Vegetation." Progress Reports RSC 1978-1 93. Texas A & M University

[21] Running, S. W., C. O. Justice, V. Salomonson, J. Barker, D. Hall, Y. J. Kaufmann, A. H. Strahler, et al. "Terrestrial Remote Sensing Science and Algorithms Planned for EOS/MODIS." International Journal of Remote Sensing, 1994, 15 (17): 3587–3620. doi:10.1080/ 01431169408954346.

[22] Huete, A. R., G. Hua, J. Qi, A. Chehbouni, and W. J. D. Van Leeuwen. "Normalization of Multidirectional Red and NIR Reflectances with the SAVI." Remote Sensing of Environment, 1992, 41 (2– 3): 143–154. doi:10.1016/0034-4257(92)90074-T

[23] Rondeaux, G., M. Steven, and F. Baret. "Optimization of Soil-Adjusted Vegetation Indices." Remote Sensing of Environment, 1996, 55 (2): 95–107. doi:10.1016/0034-4257(95)00186-7v

[24] Adamu, B., K. Tansey, and B. Ogutu. "Using Vegetation Spectral Indices to Detect Oil Pollution in the Niger Delta." Remote Sensing Letters. 2015, 6 (2): 145–154. doi:10.1080/ 2150704x.2015.1015656.

[25] Herrmann, I., A. Karnieli, D. J. Bonfil, Y. Cohen, and V. Alchanatis. "SWIR-based Spectral Indices for Assessing Nitrogen Content in Potato Fields." International Journal of Remote Sensing, 2010, 31 (19): 5127–5143. doi:10.1080/01431160903283892.

[26] Karnieli, A., Y. J. Kaufman, L. Remer, and A. Wald. "AFRI Aerosol Free Vegetation Index." Remote Sensing of Environment, 2001,77: 10–21. doi:10.1016/S0034-4257(01)00190-0.

[27] Bloomgren, S. A digital elevation model for estimating flooding scenarios at the Falsterbo Peninsula. Environmental Modelling & Software, 1999, 14(6), 579–587. doi:10.1016/s1364- 8152(99)00002-x

[28] Goudie, A. S. The drainage of Africa since the Cretaceous. Geomorphology, 2005, 67(3-4), 437– 456. doi:10.1016/j.geomorph.2004.11.008

[29] Arthur David Howard. "Drainage Analysis in Geologic Interpretation" A Summation. AAPG Bulletin, 1967, 51. doi:10.1306/5d25c26d-16c1-11d7-8645000102c1865d

[30] Hoff, R., P. Hensel, E. Proffitt, P. Delgado, G. Shigenaka, R. Yender, and A. J. Mearns. "Oil Spills in Mangroves. Planning & Response Considerations. National Oceanic and Atmospheric Administration (NOAA)." EUA. Technical Report Management: State-Of-The-Art Sensors Technology for Oil Spill Surveillance." Sensors.2002, 8 (1): 236–255. doi:10.3390/s8010236